Polymer#Grafted Nanoparticles as Single#Component, High Filler Content Composites via Simple Transformative Aging

Polymer Grafted Nanoparticles as Single Component, High Filler Content Composites via Simple Transformative Aging

*Joshua M. Kubiak and Robert J. Macfarlane**

77 Massachusetts Avenue, Cambridge, MA 02139
E-mail: rmacfarl@mit.edu

Keywords: composites, processing, nanoparticles, polymers

Polymer grafted nanoparticles (PGNPs) are ideal additives to enhance the mechanical properties and functionality of a polymer matrix and can even potentially serve as single-component building blocks for highly filled composites if the polymer content is kept low. The major challenge facing such syntheses is that PGNP-based solids with short polymer brushes often have low mechanical strength and limited processability. It therefore remains difficult to form robust architectures with a variety of 3D macroscopic shapes from single-component PGNP composites. Forming covalent bonds between crosslinkable PGNPs is a promising route for overcoming this limitation in processability and functionality, but crosslinking strategies often require careful blending of components or slow assembly methods. Here, a transformative aging strategy is presented that uses anhydride crosslinking to enable facile processing of single-component PGNP solids via thermoforming into arbitrary shapes. The use of low T_g polymer brushes enables the production of macroscopic composites with >30 vol% homogeneously distributed filler, and aging increases stiffness by 1-2 orders of magnitude. This strategy can be adapted to a variety of polymer and nanofiller compositions and is therefore a potentially versatile approach to synthesize nanocomposites that are functional, mechanically robust, and easily processable.

1. Introduction

Adding filler materials to plastics and rubbers is a common approach for improving mechanical performance[1,2] and adding or augmenting specific traits, such as thermal[3,4] or electrical conductivity.[5,6] Low aspect-ratio filler materials are typically incorporated into thermoplastic polymer matrices by mechanical or melt mixing,[7,8] though solution blending[9] and in-situ growth processes[10] can also be used. However, overcoming chemical incompatibility and ensuring a uniform distribution of filler particles is extremely difficult with these processing methods, and

significant aggregation of filler occurs at even relatively low loading due to unfavorable polymer-filler interfacial interactions.[11,12] The formation of these aggregates and agglomerates can lower the strength and toughness of the resulting composite (particularly in rigid plastics),[1] and the consequent inhomogeneity in filler distribution can interfere with filler functionality[13] or other desirable properties like optical clarity.[14] As a result, low filler loadings (typically ~20% or less) are commonly used in cases where a reduction of strength or toughness is not acceptable,[1] limiting the extent to which inorganic particles can enhance or positively impact the properties of useful composites.

Attaching polymer chains to the surfaces of the additive particles[15,16] is an attractive means of overcoming this limitation, as the polymer graft significantly reduces the interaction energy between filler and matrix. Particles with polymer chains tethered to the surface at one end to form a brush layer are often referred to as polymer grafted nanoparticles (PGNPs). PGNPs have been used as fillers to improve the mechanical,[17,18] optical,[19] electrical,[20] or thermal[21] properties of a polymer while remaining well dispersed.[22–24] The maximum filler (i.e. core particle) loading is achieved when PGNPs are used neat (without any additional matrix polymer) as a single-component or self-suspended nanocomposite.[22–24] For a given core size and grafting density, the filler loading increases with decreasing grafted chain length. However, if the grafted chains are not long enough to form interchain entanglements, bulk PGNP materials are brittle and weak, and can even exhibit poorer mechanical properties than those of the corresponding unfilled homopolymer.[25–27] Furthermore, as a result of slower polymer dynamics[23] and more colloid-like behavior[24] PGNPs with shorter polymer grafts may be more difficult to process, limiting the types of macroscopic structures that can be formed. Decreasing grafting density while maintaining chain length is another strategy for increasing core filler content.[28] Although the use of low grafting density PGNPs can mitigate poor mechanical performance, increased entanglement as well as strong interactions between grafted chains and the exposed surfaces of neighboring particles could increase the

difficulty of processing, rendering the materials difficult to use in functional applications, and this approach has not been demonstrated in bulk materials.[29,30]

An alternative method for achieving high filler content while maintaining mechanical robustness is to use short polymer grafts that contain reactive groups capable of forming covalent interparticle crosslinks; previous work has demonstrated that doing so can enhance stiffness, hardness, and damage resistance in crosslinked PGNP films, even at loadings of 40 vol% filler.[31] Similar work has demonstrated mechanical property enhancement after thermally generating crosslinks between short aliphatic capping groups.[32,33] While this covalent crosslinking strategy is promising, these materials were processed by slow drying from solution due to the fragility of the material prior to crosslinking, which limits the applicability of this approach to only thin films or coatings. Therefore, the development of a rapid and solvent-free processing method for the fabrication of low organic content PGNP solids would significantly advance the use of PGNP solids as engineering materials.

In this work, we present a transformative composite synthesis method in which rigid and highly filled composites can be produced in arbitrary geometries using typical polymer thermoforming methods. PGNPs with low glass transition temperature (T_g) polymer grafts are first formed into macroscopic shapes using hot pressing, compression molding, extrusion, or vacuum forming. The resulting soft and compliant “green” composites are then aged at elevated temperatures resulting in decomposition of the ester side chains of the monomer residues, the formation of covalent linkages between PGNPs, and depolymerization; these chemical changes simultaneously increase the filler loading of the composite and the T_g of the remaining polymer. As a result, macroscopically shaped nanocomposite materials with inorganic filler loadings up to ~35 vol% and stiffnesses several orders of magnitude higher than the initial base polymer can be readily

obtained, making this method an ideal means to achieve robust, high inorganic content composites from a single-component building block.

2. Results and Discussion

2.1 Synthesis of Polymer Grafted Nanoparticles

The development of a single component material capable of forming covalent crosslinks with itself requires the use of polymers with functional groups that can transform under appropriate external stimuli. A potentially ideal design could make use of the ester side chains present in many common polyacrylate and polymethacrylate polymers. Acrylates and methacrylates are known to undergo side chain decomposition at elevated temperatures.[34,35] The rate at which the ester side chains decompose to form acrylic or methacrylic acid residues increases with increasing length of the alkyl side chain, and the resulting acid groups react with each other in a dehydration process to yield inter- and intramolecular anhydride crosslinks. Thermal aging of acrylic polymers with long (butyl and longer) side chains yields insoluble, crosslinked solids.[36,37] However, to the best of our knowledge, this process has not been examined as a means to crosslink PGNPs, and it remains to be determined if the formation of a dense polymer brush would still permit crosslinks between adjacent particles in a composite.

To study the effect of thermal aging on PGNPs, a series of methacrylate polymers were prepared using a "grafting-from" approach via surface-initiated atom transfer radical polymerization (SI-ATRP) from initiator functionalized silica nanoparticles (SiO_2 NPs). These NPs were prepared via the Stöber method and functionalized with a silane molecule containing a bromoisobutyrate fragment for ATRP initiation. Poly(n-hexyl methacrylate) (PnHMA), poly(n-butyl methacrylate) (PnBMA), and poly(ethyl methacrylate) (PEMA) polymers were grown from these NPs (**Scheme 1** and **Figure S1**). Linear polymers without NPs were also prepared by ATRP for comparison. PGNP samples in this work are denoted by polymer type and silica content (wt%) (e.g. SiO_2-*g*-PHMA-48 has a

PnHMA graft and 48 wt% silica NPs); information for all samples used in this study is provided in **Table 1** (see Supporting Information for details on calculating PGNP parameters).

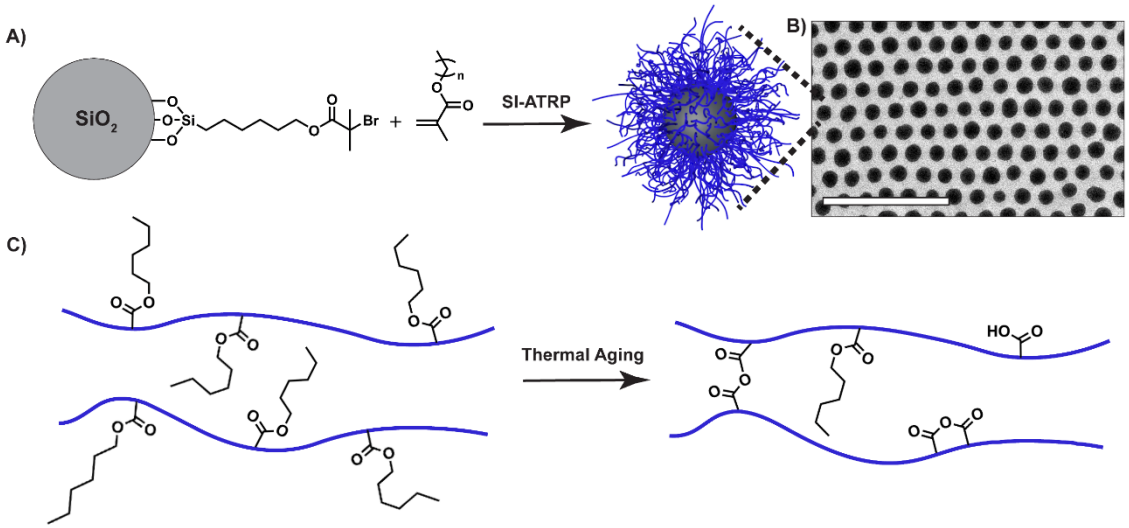

Scheme 1. A) Synthesis of polymer grafted nanoparticles (PGNPs) via ATRP of methacrylate monomers from functionalized silica NPs. B) TEM image of SiO_2-*g*-PHMA-38 (500 nm scale bar). C) Illustration of thermal aging of PnHMA resulting in the formation of anhydrides.

Sample ID	Monomer	Polymer M_n (kDa)	Polymer Đ (M_W/M_n)	NP Diameter (nm)	%SiO_2 (wt%)	Graft Density (chain/nm^2)
SiO_2-*g*-PHMA-19	nHMA	108.1	1.20	63	19.0	0.49
SiO_2-*g*-PHMA-20	nHMA	112.3	1.23	63	19.9	0.44
SiO_2-*g*-PHMA-26	nHMA	74.7	1.23	63	26.3	0.46
SiO_2-*g*-PHMA-38	nHMA	47.9	1.29	63	37.6	0.41
SiO_2-*g*-PHMA-40	nHMA	47.9	1.34	63	40.1	0.37
SiO_2-*g*-PHMA-41	nHMA	44.7	1.25	63	40.9	0.38
SiO_2-*g*-PHMA-48	nHMA	35.9	1.26	63	47.5	0.36
SiO_2-*g*-PBMA-38	nBMA	41.4	1.16	51	37.9	0.38
SiO_2-*g*-PEMA-35	EMA	45.0	1.19	51	34.9	0.47

Linear PHMA	nHMA	46.0	1.12	--	--	--
Linear PBMA	nBMA	38.0	1.07	--	--	--
Linear PEMA	EMA	37.0	1.03	--	--	--

Table 1. Composition of PGNPs and linear polymers used in this work, including number average molecular weight (Mn) and dispersity (Đ) of polymer chains and the diameter and grafting density of NP cores.

2.2 Investigation of Thermal Aging

Thermogravimetric analysis (TGA) of PGNPs (SiO_2-*g*-PHMA-38, SiO_2-*g*-PBMA-38, and SiO_2-*g*-PEMA-35) and linear polymers in air revealed that the temperature at which the polymer chains underwent substantial decomposition was elevated for PGNPs compared to linear polymers, although all grafted polymers exhibited small mass losses prior to the onset of rapid decomposition in their linear counterparts, which may be attributed to residual solvent (**Figure 1A** and **1B**). The delay in the onset of significant mass loss to over ~300 °C suggests that a processing window exists for thermoforming PGNPs below 200 °C without significantly altering the properties or behavior of the polymer chains.

Our hypothesis in this work is that the chemical transformations occurring at elevated temperatures correspond to reactions that should both remove mass associated with the organic content of the composite (increasing inorganic filler vol%) and also covalently crosslink adjacent polymer chains (which should strengthen interparticle interactions). PGNP samples (SiO_2-*g*-PHMA-38, SiO_2-*g*-PBMA-38, and SiO_2-*g*-PEMA-35) were pressed into films at 150 °C (~ 0.5 mm thick, **Figure 2A**) and heated from 50 to 200 ºC under vacuum (-30 in Hg) in an oven before releasing vacuum and continuing to age the films at 200 ºC under ambient atmosphere. The mass losses of the films were recorded, and chemical changes were monitored with attenuated total reflectance (ATR) FTIR and compared to linear polymer controls.

After 24 hrs at 200 °C, all linear polymers lost approximately 70% of their mass, while PnBMA and PnHMA PGNPs lost about 35% of their polymer mass, and the PEMA PGNP sample exhibited no loss (**Figure S2**). FTIR indicated the presence of anhydrides (peaks at 1760 and 1800 cm^{-1}) in aged linear and grafted PnBMA and PnHMA, with smaller peaks for linear PEMA, and no indication of anhydride formation in PEMA PGNPs (Figure 1C & D). In comparison, aging linear and grafted PnHMA at 150 °C under air did not result in the formation of anhydrides (**Figure S3**), and the samples exhibited significantly less mass loss (10.8% and 4.2% of polymer mass for linear PnHMA and SiO_2-*g*-PHMA-38, respectively). In all cases where anhydrides were observed, the lower wavenumber peak (1760 cm^{-1}) was more prominent than the higher wave number peak (1800 cm^{-1}) indicating that the anhydrides were primarily cyclic (i.e. formed between adjacent residues on the same chain) as expected based on prior studies. However, even a small portion of non-cyclic anhydrides has been found to render aged materials insoluble, indicating crosslinking.[37] Given that even the PGNP with the least organic content in this study (SiO_2-*g*-PHMA-48) contains nearly a million residues per particle that can participate in crosslinking (see Supporting Information), these results indicate a high likelihood of forming a percolating crosslinked network between PGNPs. Further evidence was found using solid-state ^{13}C NMR of SiO_2-*g*-PHMA-19, which revealed a composition of ~36% anhydride after 24hrs of aging based on the relative areas of the carbonyl group peaks (**Figure S4**). Importantly, this significant fraction of transformed methacrylate monomers indicates that the aging process occurred throughout the film and was not localized to the surface.[38] Collectively, these results demonstrate that it is possible to thermally age PGNPs with low T_g methacrylic grafted chains resulting in the formation of anhydride linkages and a reduction of the organic component of the composite.

Notably, PnHMA PGNPs and linear polymer cured at 200 ºC for 24 hrs under vacuum also did not form significant anhydrides (**Figure S5**). These data indicate that anhydride formation and depolymerization are significantly accelerated by the presence of air, but slow aging is possible

below the onset of rapid decomposition. To further support these hypotheses regarding the chemical transformations occurring during thermal aging, a mass spectrometer coupled to TGA was used to determine the masses of the reaction products being lost during thermal aging of SiO_2-*g*-PHMA-19 at 200 °C in air. Fragments were detected that were characteristic of the alcohol or alkene fragments that would be expected from ester decomposition, as well as fragments characteristic of the monomer due to depolymerization, (**Figure S6**) with no such fragments or mass loss observed under a helium atmosphere. This finding is particularly important to the development of aging procedures given the wide range of temperatures and environments present in the existing literature and the postulation of both aerobic and anaerobic mechanisms for the aging of polymethacrylate materials.[38]

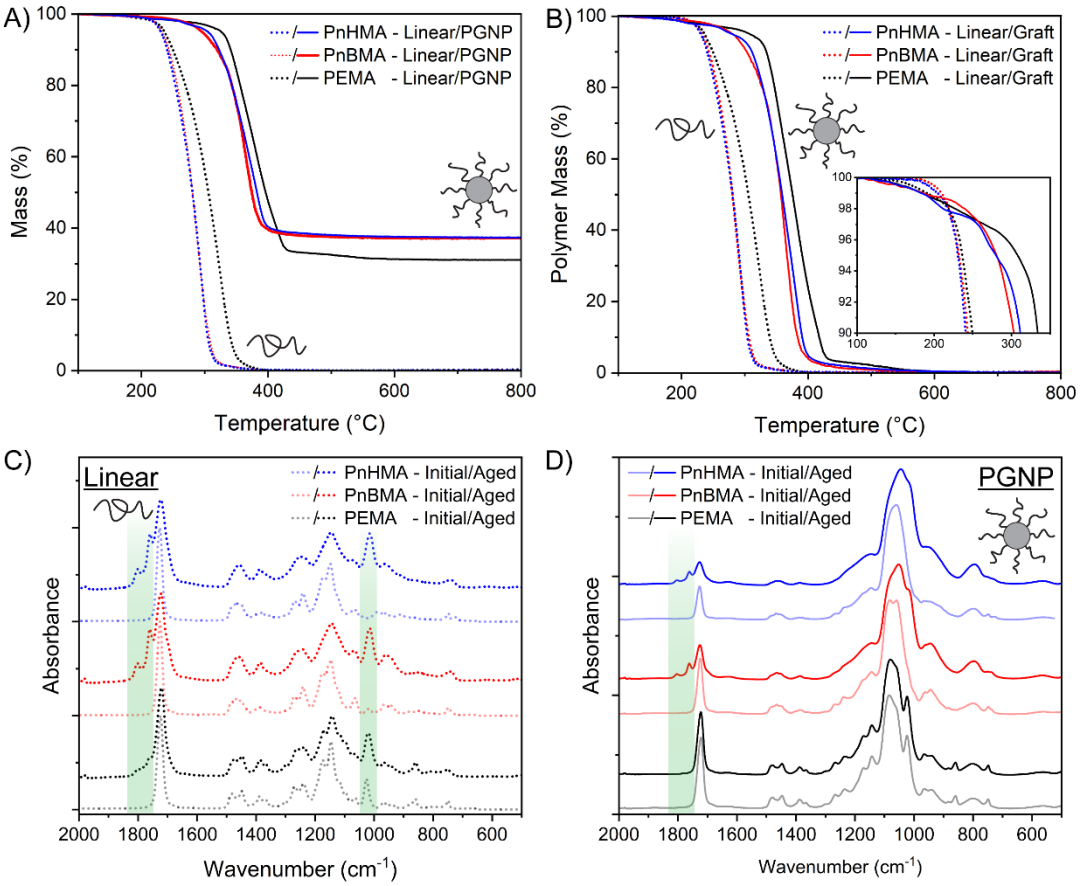

Figure 1. A) TGA of linear polymers and PGNPs (SiO_2-*g*-PHMA-38, SiO_2-*g*-PBMA-38, and SiO_2-*g*-PEMA-35) in air showing higher decomposition temperature for PGNPs. B) TGA data replotted normalizing PGNPs by their polymer content. C) and D) ATR FTIR of linear polymers and PGNPs, respectively, before and after aging for 24 hrs at 200 °C in air. The highlighted regions indicate peaks corresponding to anhydride stretches.

2.3 Effects of Aging on Single-Component Composite Films

In order to determine the compositional limits of the aging process and investigate whether or not filler loading plays a role in aging, a series of PnHMA PGNPs were synthesized with varying lengths of grafted chains chosen such that the silica fraction ranged from ~20 to 50 wt%. PnHMA was selected because the lower T_g polymer facilitated thermal processing. These samples were pressed at 150 °C into ~0.5 mm thick free-standing films, and portions of the films were aged in air at 200 °C for varying lengths of time up to 24 hrs (Figure 2E).

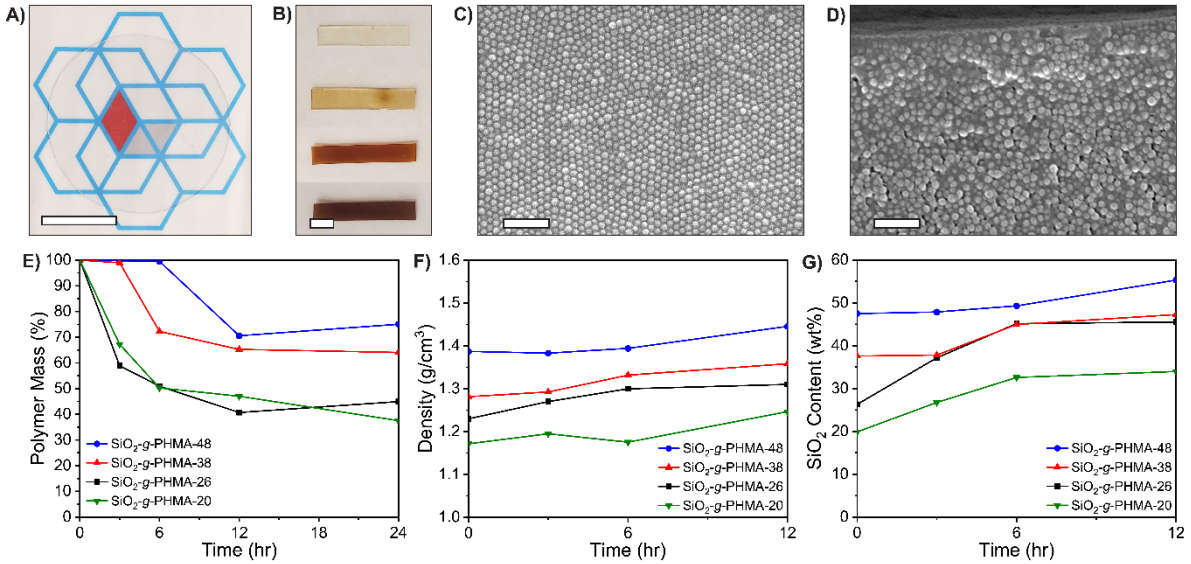

Figure 2. A) Approx. 0.5 mm thick film of SiO_2-*g*-PHMA-20 after hot pressing (scale bar is 20 mm) B) Color change in rectangular films of SiO_2-*g*-PHMA-38 aged for 0h, 3h, 6h, and 12h from top to bottom (scale bar is 5 mm) C) and D) SEM images of the face and microtomed cross-section, repsectively, of a pressed film of SiO_2-*g*-PHMA-38 after 12h of aging (scale bars are 500 nm). E), F), and G) change in polymer content, density, and filler loading, respectively, for PnHMA PGNPs as a function of aging time.

As samples were aged, the films transitioned from a flexible, tacky material into a more rigid composite, with little change in mass after 12 hrs. Samples with a lower filler content were found to undergo aging faster (as indicated by a more rapid weight loss), and also exhibit a larger increase in silica content (Figure 2E and 2G). In addition, during aging, the samples change from nearly colorless to a deep reddish brown, which is attributed to the oxidation of residual copper from the polymerization that was difficult to fully remove due to the porous nature of the silica particles (Figure 2B and **Figure S7**).[39,40] Importantly, the color change could in principle be eliminated by using less porous particles or by synthesizing the polymers using metal-free ATRP [41]; these studies will be the focus of future investigations.

An important question regarding the thermal aging of PGNPs is whether or not the samples remain dense during polymer decomposition, or if this process results in void spaces. Sample dimensions and masses were used to calculate approximate densities as a function of thermal treatment (Figure 2F), and density was found to increase during aging. In addition, SEM imaging of the surfaces of films cured for 12 hrs showed no evidence of microscopic porosity at the surface (Figure 2C and **Figure S8**). Small defects are visible in cross-sections of cured films prepared by cryo-microtome, but these may be an artifact of the cutting process (Figure 2D and Figure S8).[42] In general, no evidence of large voids was found, suggesting that the films remained dense throughout the aging process. Furthermore, small-angle X-ray scattering (SAXS) experiments showed a decrease in interparticle spacing (shift of primary peak to higher q) for all samples after aging for 12 hrs, without significant peak broadening, which is also consistent with densification of the composites (**Figure S9** and **Table S1**).

To further probe the stability of these materials post thermal treatment, samples of aged PGNPs were soaked in methyl ethyl ketone (MEK) to evaluate the effects of aging on solubility. After 1 week of gentle shaking at room temperature followed by 1 minute of sonication, all of the “green”

samples were either completely or mostly dissolved (**Figure S10**). In contrast, after aging past the point at which each material began to undergo significant mass loss, the samples remained mostly intact during the test, with all samples that were aged for 12 hrs showing minimal dissolution. This decrease in solubility presents further evidence of the formation of interchain covalent crosslinks that increase the strength of interparticle interactions. In all, these results show that bulk methacrylate-based PGNPs can undergo a thermal aging process that transforms the material from a soft, soluble, and easily formable "green" state into a rigid and crosslinked plastic. Moreover, this transformation was performed without affecting the distribution of particles within the material, as evidenced by the microscopy images and x-ray scattering data. As a result, it was hypothesized that these films should have significantly improved mechanical performance due to the thermal aging process.

2.4 Mechanical Properties of Aged Composites

Alteration of composite mechanical behavior due to thermal aging was investigated by temperature-controlled dynamic mechanical analysis (DMA) of rectangular film specimens. Films were evaluated in tension (0.1% strain (0.05% for SiO_2-*g*-PHMA-48), 1Hz, 2 °C/min) from -40 to 200 ºC to examine behavior both above and below the T_g of PnHMA (-5 ºC for the linear polymer).[43] Only a single sample was measured at each condition given the variation in the rate of transformation during aging exacerbated by small variations in initial film thickness and heat distribution in the aging oven; future studies will evaluate the progression of aging as a function of film thickness using a convection oven for more consistent heating.

The elastic storage modulus (E') and loss factor (Tan δ) are presented in **Figure 3** for each material as a function of the remaining polymer content after aging (aged samples with insignificant mass loss are neglected). In all "green" samples, there was a large peak in loss factor at a temperature of 23-25 ºC that corresponds to the glass transition of PnHMA. The peak in Tan δ is

generally a higher measurement of T_g; a more representative measurement is a peak in loss modulus (E'') which is observed between 1-7 ºC (**Table S2** and **Figure S11**) for the uncured samples. At 25 °C, "green" samples had storage moduli of 17, 22, 29, and 47 MPa for SiO_2-*g*-PHMA-20, -26, -38, and -48, respectively, which is similar to the reported value of 25 MPa for linear PnHMA.[44] As aging progressed, the initial peak in loss factor diminished and shifted to higher temperatures, and, simultaneously, a new peak appeared at higher temperatures (104-106 ºC) which also diminished and shifted to higher temperatures with continued aging. This second peak in loss tangent was attributed to the formation of poly(methyl anhydride) (T_g ~159 °C) resulting from ester side chain decomposition.[45] A corresponding peak in E'' is not observed, although the initial peak broadens significantly and shifts to higher temperatures (10-34 ºC).

As aging progressed, dramatic increases in storage modulus were observed between 25 and 100 ºC. At room temperature (25 ºC), the storage moduli for 12 hr aged samples increased to ~69x, 81x, 43x, and 28x their initial values for SiO_2-*g*-PHMA-20, -26, -38, and -48 samples, respectively. At 50 °C, these figures were increased to ~165x, 189x, 61x and 50x, respectively (**Table S3**). Across all samples, the temperature above which E' falls below 1 GPa increased from -11 to -2 ºC to 31 to 41 ºC (Table S4). These massive increases in modulus indicate that aging transforms the initially malleable composite into a rigid material at typical operating temperatures, and these large increases cannot be explained by an increase in organic content due to de-polymerization alone, indicating that partial conversion of ester side-chains to anhydrides occurs throughout the material. Samples aged for 12 hours also had a higher plateau modulus at higher temperatures, providing another indication of crosslinking.

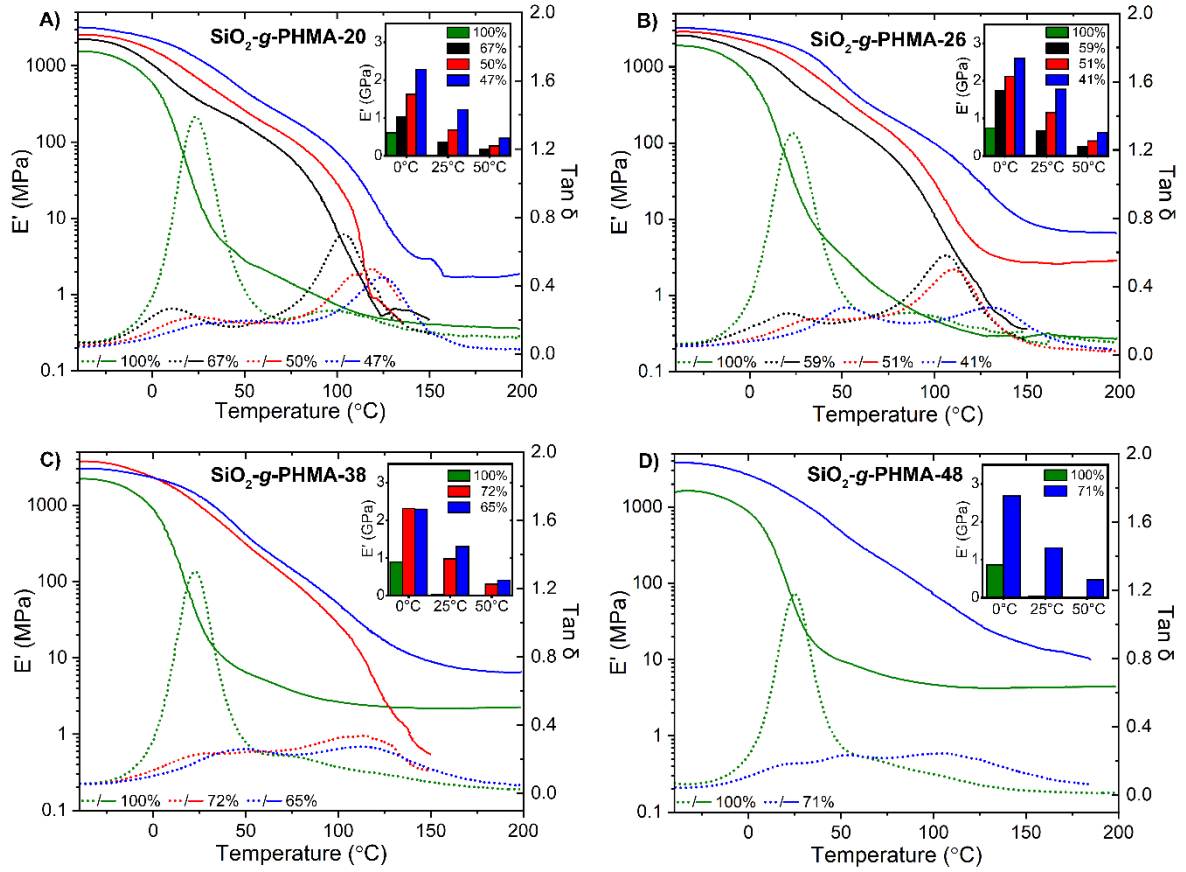

Figure 3. DMA temperature-sweep of aged PnHMA PGNPs. Green, black, red, and blue curves indicate samples which were aged for 0 hrs, 3 hrs, 6 hrs, and 12 hrs, respectively. Solid lines show storage modulus (E') and dashed lines show loss factor (Tan δ). Insets compare E' on a linear axis at selected temperatures. Key indicates remaining percentage of polymer mass in the composites.

To demonstrate that aging is applicable to a range of methacrylate PGNPs, smaller samples of SiO_2-*g*-PBMA-38 and SiO_2-*g*-PEMA-35 composites were analyzed via nanoindentation to measure the reduced elastic modulus (E_r) and hardness (H) as a function of aging time. While the requisite aging times were longer, significant enhancements in stiffness and hardness, which is correlated to strength, were realized for both polymers (see **Figure S12**). As expected given the lower starting values and faster aging for longer ester side chains, the improvements were more drastic for the PBMA PGNPs, with modulus increasing from 1.28 ± 0.03 GPa to 8.9 ± 0.3 GPa and hardness from 20.7 ± 0.7 MPa to 361 ± 21 MPa after aging for 72 hrs. These significant improvements indicate the generality of this approach to PGNPs with varying graft compositions.

2.5 Demonstration of Formability

To date, investigations into the use of neat PGNPs as engineering materials have largely focused on thin films (often supported by a substrate), which is a limiting factor in their application. To further demonstrate the utility of this novel method for processing rigid composites with a high fraction of evenly dispersed filler particles, samples of SiO_2-*g*-PHMA were shaped via common thermoforming methods to produce macroscopic 3D shapes (**Figure 4**). Approximately 1 gram of SiO_2-*g*-PHMA-41 was compression molded at 150 ºC in a PFTE mold to form a freestanding copy of our university logo. In another example, SiO_2-*g*-PHMA-40 was extruded at ~190 °C with a ~4:1 diameter reduction to form a 2 mm diameter composite column. Lastly a ~0.5 mm sheet of SiO_2-*g*-PHMA-20 was prepared as before by hot pressing and then subsequently vacuum formed to produce a small dome over a PTFE mold.

The dome and column were aged at 200 °C for 12 hours to yield a rigid composite, while the logo was aged for 48 hours. Silica content increased from 41, 40, and 20 wt% to 49, 45, and 34 wt% for the logo, column, and dome, respectively (**Figure S13**). It was found that curing progressed more slowly for the thicker logo and column shapes (see mass loss in Figure S13), but, in all cases, SEM imaging of the aged structures showed that the dense arrangement of nanoparticles separated by polymer shells was maintained.

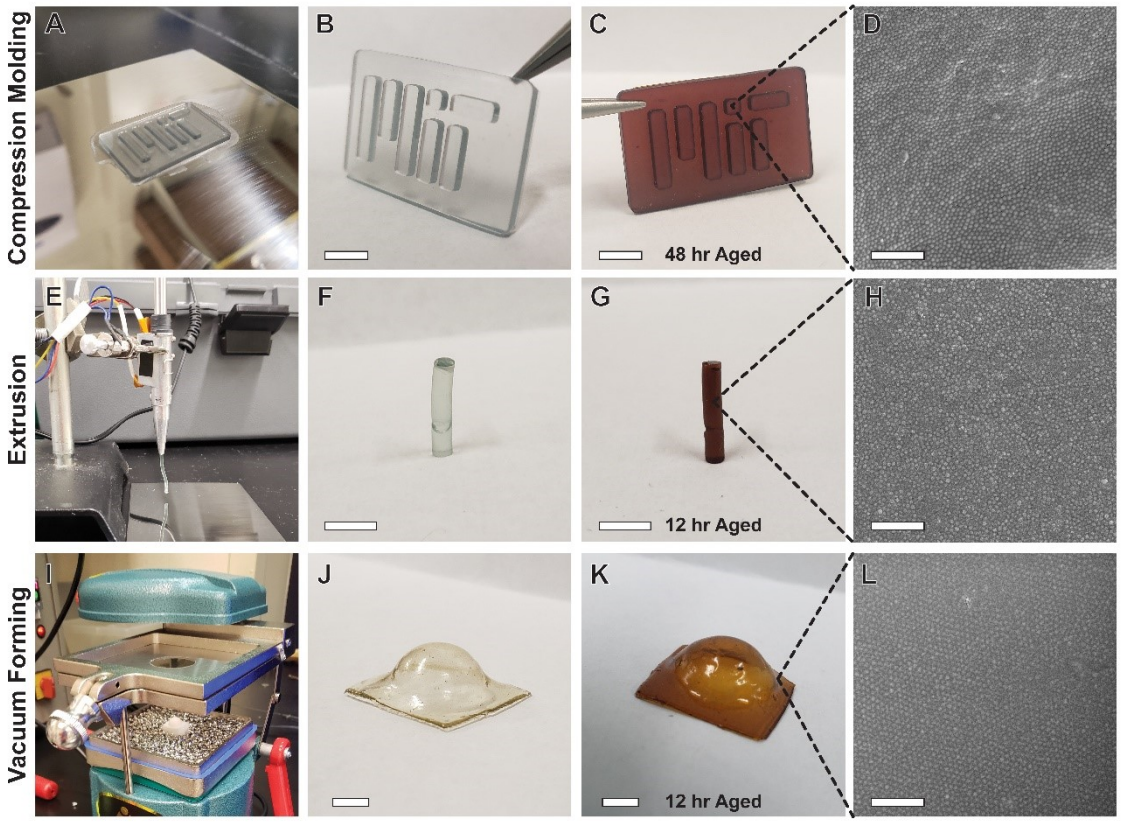

Figure 4. A) – C) Compression molding of SiO_2-*g*-PHMA-41 into freestanding university logo in a PTFE mold and subsequent thermal aging. D) SEM of logo after 48 hrs of aging. E) – F) Extrusion of SiO_2-*g*-PHMA-40 into a ~ 2mm diameter filament and subsequent thermal aging. G) SEM of radial surface of filament after 12 hrs of aging. I) – K) Vacuum forming of SiO_2-*g*-PHMA-20 into a dome shape and subsequent thermal aging. L) SEM of edge of dome after 12 hrs of aging. Scale bars are approx. 5 mm for optical images and are 1 µm for SEM.

3. Conclusions

Transformative thermal aging of PGNPs shows significant potential as a route to produce highly-filled composites while maintaining the processing advantages of thermoplastic materials. Although anhydride formation has been investigated for linear polymers, the PGNP architecture allows for uniform filler distribution with no aggregation or mixing steps. Additional investigations are warranted into optimizing aging conditions, examining how the amount of filler content affects deformation during aging, and thoroughly analyzing composite mechanical properties. Furthermore, the use of functional filler materials (e.g. alumina or boron nitride for thermal conductivity,[4] barium

titanate for permittivity,[46] titania for refractive index[47]) has the potential to make this composite synthesis method widely applicable to a variety of useful applications including coatings, structural materials, or interfacial materials. Using this approach, a particle composition can be selected to yield a desired property and then grafted with a commercially available methacrylate polymer using established polymerization or grafting methods to yield a low T_g single-component composite material. The material can then shaped by traditional polymer thermoforming methods into whatever geometry is necessary for the application, and the "green" part subsequently aged at elevated temperatures to yield a rigid composite with a higher filler loading and elevated functionality. This new method combines the rapid processability of polymers with the wide range of utility of inorganic materials and represents a significant step towards the application of PGNPs as designer composites.

4. Experimental Section

Chemicals were purchased from Fisher or Alfa Asear. Monomers were filtered through a plug of basic alumina and stored in a freezer prior to use. All other chemicals were used as received. Pressed samples were stored under vacuum until used.

Silica Synthesis: Silica nanoparticles were prepared via the Stöber method and then immediately functionalized with (2-bromo-2-methyl)propionyloxyhexyltriethoxysilane (BHE) in the same flask as reported previously.[31] Particles were purified by repeated centrifugation and kept as a stock solution in anisole.

Polymerization: In a typical PGNP synthesis, 7.4 g of 6.5 wt% SiO_2-BHE NP solution in anisole (19 µmol), 14.9 mL of n-hexyl methacrylate (76 mmol), 3.4 mg $CuBr_2$ (as a 20mg/mL solution in DMF; 15 µmol), 16 µL of pentamethyldiethylenetriamine (PMDETA) (76 µmol), and 8 mL of anisole (50 vol%) were combined in a 50 mL Schlenk flask. The flask was degassed by five freeze-pump-thaw cycles

prior to backfilling with N_2 gas. A N_2 purged solution of tin(II) 2-ethylhexanoate ($Sn(EH)_2$) in anisole (20.45 mg/mL) was injected into the flask via a N_2 purged needle (0.3 mL; 15 µmol). The flask was then lowered into a 60 ºC oil bath, and the reaction mixture was magnetically stirred. Reaction progress was monitored by removing small aliquots via N_2 purged syringe and measuring the wt% of solids using an analytical balance. The reaction was quenched at a desired conversion by cooling in liquid nitrogen and opening to air. PGNPs were purified by precipitation into methanol, followed by three cycles of centrifugation and dispersion in methyl ethyl ketone (MEK) and a final precipitation in methanol. The purified material was dried under vacuum to <100 mTorr at 50 ºC. In a typical linear polymer synthesis, 6.2 µL of ethyl bromoisobutyrate (42 µmol), 8.3 mL of n-hexyl methacrylate (42 mmol), 0.25 mg $CuBr_2$ (as a 20 mg/mL solution in DMF; 21 µmol), 6.7 µL of hexamethyltriethylenetetramine (HMTETA) (23 µmol), and 16.7 mL of anisole (67 vol%) were combined in a 50 mL Schlenk flask which was degassed by four freeze-pump-thaw cycles. On the last cycle, the flask was backfilled with N_2 while frozen, and 3.0 mg (21 µmol) of CuBr was added while purging the flask with N_2. The flask was then resealed, cycled between vacuum and N_2 three times, and placed in an oil bath at 50 ºC. Reaction progress was monitored by tracking the monomer to solvent ratio with ^{1}H NMR. The reaction was quenched by cooling with liquid nitrogen and opening to air, and the product was purified by three cycles of precipitation in methanol and redispersion in MEK, followed by drying under vacuum. PGNPs and linear polymers using other monomers were prepared in the same way.

GPC: Samples were prepared for GPC by etching ~ 25 mg of PGNP in a solution of 2:1 THF/HF overnight (~3 mL). The etching solution was quenched with ammonia solution (28%) while frozen with liquid nitrogen, and the organic layer was removed after thawing and dried over magnesium sulfate. Samples were analyzed using an Agilent 1260 Infinity II system with a multidetector suite equipped with two sequential Agilent ResiPore columns using a THF eluent at 40 ºC with a flow rate of 1 mL/min. Absolute molecular weights were determined using refractive index and right-angle

light scattering (RALS) detectors. Incremental refractive index (dn/dc) values of 0.076, 0.078, and 0.071 mL/g were used for PEMA, PnBMA, and PnHMA, respectively, as measured with linear polymer samples. For most etched samples, a high molecular weight shoulder was observed, which was attributed to either incomplete etching given the non-polar nature of hexyl methacrylate or to termination by coupling during polymerization.

Sample Pressing: PGNP films were prepared by pressing on a Carver 4386 press at 150 °C between mirror-finish stainless-steel plates separated by a 0.5 mm ring shim at a maximum load of ~1000 kg. Samples were warmed in the press for 2 min prior to pressing. The press was water-cooled to room temperature in ~15 minutes before removing samples. The resulting flexible disks were cut into ~4 mm x 20 mm strips for DMA using a set of parallel razor blades. Smaller pieces for chemical analyses were also cut using a razor blade.

Sample Curing: Samples were placed on a stainless-steel plate covered with an adhesive PTFE film that was loaded into a vacuum oven at 50 °C. While under vacuum, the temperature was ramped to 200 °C over ~1 hr at -30 in Hg. At 200 °C, vacuum was released, and aging was continued under ambient atmosphere with inlet and outlet valves open. Control samples (0 hr) were removed immediately upon releasing vacuum.

TGA: Sample composition and degradation temperatures were determined using a TA Instruments Discovery TGA with high-temperature platinum pans. Composition measurements were performed on precipitated PGNPs under N_2 gas with a 15 min hold at 150 °C before heating to 800 °C at 15 °C/min. Decomposition measurements were performed on pressed films under air with a 15 min hold at 100 °C before heating to 800 °C at 10 °C/min. For mass spectrometry of evolved gasses, a Pfeiffer Vacuum ThermoStar was used with a capillary inserted into the evolved gas heater of the TGA, a scan window from 30-90 m/z, and the slowest available scan rate (1 (m/z)/s).

FTIR: ATR FTIR was performed on a Nicolet iS50 spectrometer from 4000-525 cm^{-1} using a diamond window, 128 scans, and automatic baseline and ATR correction.

DMA: DMA was conducted on a TA Instruments Q850 with a liquid nitrogen gas cooling accessory. Measurements were conducted using a film tension clamp at a dynamic strain of +/- 0.1% (0.05% for 50 wt% SiO_2 samples) at 1 Hz from -40 °C to 200 °C at a heating rate of 2 ºC/min. A 0.1 N pre-load was applied with 125% force tracking to minimize creep. Film thickness was measured using a calibrated film thickness gauge or micrometer, and width was measured with digital calipers.

TEM: TEM samples were prepared by drop casting a ~1 mg/mL solution of PGNPs in toluene onto water in a covered petri dish. After evaporation of the toluene, a carbon-coated copper TEM grid was used to scoop a layer of PGNPs from the surface of the water. Grids were imaged using an FEI Tecnai (G2 Spirit TWIN) digital TEM with an accelerating voltage of 120 kV.

SEM: SEM samples were coated with ~8 nm of gold using a Quorum Technologies SC7640 sputter coater. Images were taken on a Zeiss Sigma 300 VP field emission SEM at 10kV with an in-lens secondary electron detector. Cross-sections were first cut with a razor blade before being cut more-smoothly on a Lecia cryo-microtome using a glass knife at -50 °C.

Nanoindentation: Nanoindentation was performed using a Hysitron Triboindenter with a diamond berkovich tip using a tip area function determined from indentation of fused quartz. An array of 7 x 7 indents was made in each sample in depth-control mode up to 800 nm. Indentation and withdrawal rates of 40 nm/s were used, with a 20 s hold at peak depth for stress relaxation. Reduced modulus and hardness were calculated from the load-depth data by Oliver-Pharr[48] analysis in MATLAB using a rate-jump method[49–51] with power function fits to both the relaxation and withdrawal segments. A plastic contact assumption was found to be appropriate for all samples.[50]

Supporting Information

Supporting Information is available from the Wiley Online Library or from the author.

SEM and TEM images of PGNPs, additional aging condition test data, tabulated mechanical data, dissolution test, nanoindentation data, and details of PGNP composition calculations.

Acknowledgements

This work was primarily supported by an NSF CAREER grant, award number CHE-1653289. J.M.K. was supported by a National Defense Science and Engineering Graduate (NDSEG) Fellowship. This work made use of the MRSEC Shared Experimental Facilities at MIT, supported by the NSF under Award DMR-1419807. SAXS experiments at beamline 12-ID-B at the Advanced Photon Source at Argonne National Laboratory were supported by the U.S. Department of Energy, Office of Science, Office of Basic Energy Sciences, under Contract DE-AC02-06CH11357.

Received: ((will be filled in by the editorial staff))
Revised: ((will be filled in by the editorial staff))
Published online: ((will be filled in by the editorial staff))

References

[1] S.-Y. Fu, X.-Q. Feng, B. Lauke, Y.-W. Mai, *Compos. Part B Eng.* **2008**, *39*, 933.

[2] E. Y. Lin, A. L. Frischknecht, R. A. Riggleman, *Macromolecules* **2020**, acs.macromol.9b02733.

[3] Y. Agari, A. Ueda, S. Nagai, *J. Appl. Polym. Sci.* **1993**, *49*, 1625.

[4] H. Chen, V. V. Ginzburg, J. Yang, Y. Yang, W. Liu, Y. Huang, L. Du, B. Chen, *Prog. Polym. Sci.* **2016**, *59*, 41.

[5] P. Ghosh, A. Chakrabarti, *Eur. Polym. J.* **2000**, *36*, 1043.

[6] W. Zheng, S.-C. Wong, *Compos. Sci. Technol.* **2003**, *63*, 225.

[7] F. P. L. Mantia, M. Morreale, Z. A. M. Ishak, *J. Appl. Polym. Sci.* **2005**, *96*, 1906.

[8] W. Yan, R. J. T. Lin, D. Bhattacharyya, *Compos. Sci. Technol.* **2006**, *66*, 2080.

[9] P. Joseph, *Compos. Sci. Technol.* **1999**, *59*, 1625.

[10] Q. Zhou, Z. Bai, W. Lu, Y. Wang, B. Zou, H. Zhong, *Adv. Mater.* **2016**, *28*, 9163.

[11] T. Jesionowski, K. Bula, J. Janiszewski, J. Jurga, *Compos. Interfaces* **2003**, *10*, 225.

[12] Y. Zare, *Compos. Part Appl. Sci. Manuf.* **2016**, *84*, 158.

[13] A. C. Balazs, T. Emrick, T. P. Russell, *Science* **2006**, *314*, 1107.

[14] J. Loste, J.-M. Lopez-Cuesta, L. Billon, H. Garay, M. Save, *Prog. Polym. Sci.* **2019**, *89*, 133.

[15] M. K. Corbierre, N. S. Cameron, M. Sutton, K. Laaziri, R. B. Lennox, *Langmuir* **2005**, *21*, 6063.

[16] C. Chevigny, F. Dalmas, E. Di Cola, D. Gigmes, D. Bertin, F. Boué, J. Jestin, *Macromolecules* **2011**, *44*, 122.

[17] T. Shah, C. Gupta, R. L. Ferebee, M. R. Bockstaller, N. R. Washburn, *Polymer* **2015**, *72*, 406.

[18] M. Giovino, J. Pribyl, B. Benicewicz, R. Bucinell, L. Schadler, *Nanocomposites* **2018**, *4*, 244.

[19] Z. Wang, Z. Lu, C. Mahoney, J. Yan, R. Ferebee, D. Luo, K. Matyjaszewski, M. R. Bockstaller, *ACS Appl. Mater. Interfaces* **2017**, *9*, 7515.

[20] C. A. Grabowski, H. Koerner, J. S. Meth, A. Dang, C. M. Hui, K. Matyjaszewski, M. R. Bockstaller, M. F. Durstock, R. A. Vaia, *ACS Appl. Mater. Interfaces* **2014**, *6*, 21500.

[21] C. Mahoney, C. M. Hui, S. Majumdar, Z. Wang, J. A. Malen, M. N. Tchoul, K. Matyjaszewski, M. R. Bockstaller, *Polymer* **2016**, *93*, 72.

[22] N. J. Fernandes, H. Koerner, E. P. Giannelis, R. A. Vaia, *MRS Commun.* **2013**, *3*, 13.

[23] S. Srivastava, S. Choudhury, A. Agrawal, L. A. Archer, *Curr. Opin. Chem. Eng.* **2017**, *16*, 92.

[24] C. R. Bilchak, Y. Huang, B. C. Benicewicz, C. J. Durning, S. K. Kumar, *ACS Macro Lett.* **2019**, *8*, 294.

[25] J. Choi, C. M. Hui, J. Pietrasik, H. Dong, K. Matyjaszewski, M. R. Bockstaller, *Soft Matter* **2012**, *8*, 4072.

[26] M. Schmitt, J. Choi, C. Min Hui, B. Chen, E. Korkmaz, J. Yan, S. Margel, O. Burak Ozdoganlar, K. Matyjaszewski, M. R. Bockstaller, *Soft Matter* **2016**, *12*, 3527.

[27] N. K. Hansoge, T. Huang, R. Sinko, W. Xia, W. Chen, S. Keten, *ACS Nano* **2018**, *12*, 7946.

[28] J. Midya, Y. Cang, S. A. Egorov, K. Matyjaszewski, M. R. Bockstaller, A. Nikoubashman, G. Fytas, *Nano Lett.* **2019**, *19*, 2715.

[29] S. Choudhury, A. Agrawal, S. A. Kim, L. A. Archer, *Langmuir* **2015**, *31*, 3222.

[30] A. Agrawal, H.-Y. Yu, A. Sagar, S. Choudhury, L. A. Archer, *Macromolecules* **2016**, *49*, 8738.

[31] J. M. Kubiak, R. J. Macfarlane, *Adv. Funct. Mater.* **2019**, *29*, 1905168.

[32] B. Domènech, A. T. L. Tan, H. Jelitto, E. Z. Berodt, M. Blankenburg, O. Focke, J. Cann, C. C. Tasan, L. C. Ciacchi, M. Müller, K. P. Furlan, A. J. Hart, G. A. Schneider, *Adv. Eng. Mater.* **2020**, adem.202000352.

[33] A. Dreyer, A. Feld, A. Kornowski, E. D. Yilmaz, H. Noei, A. Meyer, T. Krekeler, C. Jiao, A. Stierle, V. Abetz, H. Weller, G. A. Schneider, *Nat. Mater.* **2016**, *15*, 522.

[34] A. H. Soeriyadi, V. Trouillet, F. Bennet, M. Bruns, M. R. Whittaker, C. Boyer, P. J. Barker, T. P. Davis, C. Barner-Kowollik, *J. Polym. Sci. Part Polym. Chem.* **2012**, *50*, 1801.

[35] M. Lazzari, O. Chiantore, *Polymer* **2000**, *41*, 6447.

[36] H. Ha, K. Shanmuganathan, C. J. Ellison, *ACS Appl. Mater. Interfaces* **2015**, *7*, 6220.

[37] N. Grassie, J. R. MacCallum, *J. Polym. Sci. A* **1964**, *2*, 983.

[38] L. J. Mathias, Ed. , *Solid State NMR of Polymers*, Springer US, Boston, MA, **1991**.

[39] S. Li, Q. Wan, Z. Qin, Y. Fu, Y. Gu, *Langmuir* **2015**, *31*, 824.

[40] C. A. R. Costa, C. A. P. Leite, F. Galembeck, *Langmuir* **2006**, *22*, 7159.

[41] J. Yan, X. Pan, M. Schmitt, Z. Wang, M. R. Bockstaller, K. Matyjaszewski, *ACS Macro Lett.* **2016**, *5*, 661.

[42] M. Michel, H. Gnägi, M. Müller, *J. Microsc.* **1992**, *166*, 43.

[43] W. C. Child, J. D. Ferry, *J. Colloid Sci.* **1957**, *12*, 389.

[44] C. Heinzmann, U. Salz, N. Moszner, G. L. Fiore, C. Weder, *ACS Appl. Mater. Interfaces* **2015**, *7*, 13395.

[45] B.-C. Ho, Y.-D. Lee, W.-K. Chin, *J. Polym. Sci. Part Polym. Chem.* **1992**, *30*, 2389.

[46] Z.-M. Dang, J.-K. Yuan, J.-W. Zha, T. Zhou, S.-T. Li, G.-H. Hu, *Prog. Mater. Sci.* **2012**, *57*, 660.

[47] C. Lü, B. Yang, *J. Mater. Chem.* **2009**, *19*, 2884.

[48] W. C. Oliver, G. M. Pharr, *J. Mater. Res.* **2004**, *19*, 3.

[49] A. H. W. Ngan, B. Tang, *J. Mater. Res.* **2009**, *24*, 853.

[50] N. Fujisawa, M. V. Swain, *J. Mater. Res.* **2006**, *21*, 708.

[51] B. Tang, A. H. W. Ngan, *J. Mater. Res.* **2003**, *18*, 1141.

The use of polymer-grafted nanoparticles (PGNPs) as a single-component composite provides control over material composition, structure, and properties. However, maximizing filler loading without compromising mechanical integrity or processability remains a challenge. Herein, the thermal crosslinking of ester groups in soft methacrylic polymers is developed as generalizable method for synthesizing rigid, highly-filled nanocomposites that can be easily formed into macroscopic structures.

Keyword: composites

J. M. Kubiak, R. J. Macfarlane*

Polymer Grafted Nanoparticles as Single Component, High Filler Content Composites via Simple Transformative Aging